Direct Trajectory Optimization and Costate Estimation via an Orthogonal Collocation Method

Article *in* Journal of Guidance, Control, and Dynamics · August 2006

DOI: 10.2514/1.20478

4 authors:

David A. Benson
Draper Laboratory

Geoffrey T. Huntington
Blue Origin

Tom Thorvaldsen
Draper Laboratory

Anil V. Rao
University of Florida

JOURNAL OF GUIDANCE, CONTROL, AND DYNAMICS
Vol. 29, No. 6, November–December 2006

Engineering Notes

ENGINEERING NOTES are short manuscripts describing new developments or important results of a preliminary nature. These Notes should not exceed 2500 words (where a figure or table counts as 200 words). Following informal review by the Editors, they may be published within a few months of the date of receipt. Style requirements are the same as for regular contributions (see inside back cover).

Direct Trajectory Optimization and Costate Estimation via an Orthogonal Collocation Method

David A. Benson,* Geoffrey T. Huntington,† Tom P. Thorvaldsen,‡ and Anil V. Rao§
Charles Stark Draper Laboratory, Inc., Cambridge, Massachusetts 02139

DOI: 10.2514/1.20478

I. Introduction

NUMERICAL methods for solving optimal control problems fall into two general categories: indirect methods and direct methods [1]. In an indirect method, first-order necessary conditions for optimality are derived from the optimal control problem via the calculus of variations. These necessary conditions form a Hamiltonian boundary-value problem (HBVP), which is then solved (often numerically) for extremal trajectories [2]. The optimal solution is then found by choosing the extremal trajectory with the lowest cost. The primary advantages of indirect methods are their high accuracy in the solution and the assurance that the solution satisfies the first-order optimality conditions. However, indirect methods have several disadvantages, including small radii of convergence, the need to analytically derive the HBVP, a (generally nonintuitive) initial guess for the costate, and if path constraints are present, a priori knowledge of the constrained and unconstrained arcs.

In a direct method, the continuous-time optimal control problem is transcribed to a nonlinear programming problem (NLP). The resulting NLP can be solved numerically by well-developed algorithms, which attempt to satisfy a set of conditions [called Karush–Kuhn–Tucker (KKT) conditions] associated with the NLP. Although direct methods do not suffer from the disadvantages of the indirect approach, many provide either an inaccurate costate or no costate information whatsoever. There are several methods to transcribe an optimal control problem into an NLP: examples include direct shooting methods [3], state and control parameterization methods [4–6], and pseudospectral methods [7–10]. In a direct shooting method, the control alone is parameterized and explicit numerical integration is used to satisfy the differential constraints. In a state and control parameterization method, piecewise polynomials are used to approximate the differential equations at collocation points. State and control parameterization methods have the advantage that they avoid the numerically expensive explicit integration of control parameterization methods. In a pseudospectral method, the state and control are parameterized using global polynomials, and the differential-algebraic equations are approximated via orthogonal collocation. Pseudospectral methods are based on spectral methods which were traditionally used to solve fluid dynamics problems and typically have faster convergence rates than other methods [11,12]. Pseudospectral methods have been applied to optimal control problems in the 1980s using Chebyshev polynomials [7,8]. Within the aerospace community, two well-known pseudospectral methods for solving optimal control problems are the Legendre pseudospectral method [9] and the Chebyshev pseudospectral method [10]. Additionally, a costate estimation procedure that uses the Legendre pseudospectral method was developed in [13,14].

Interestingly, a significant amount of work in pseudospectral methods has also been done in the chemical engineering community that makes the distinction between state and control parameterization methods and pseudospectral methods less clear. A groundbreaking work by Reddien [15] approximated the state with splines and performed collocation at the Legendre–Gauss (LG) (also referred to as Gauss) points as early as 1979. This paper also analytically proved convergence of the method and showed the equivalence between the KKT conditions and the first-order optimality conditions for a simple problem. Cuthrell and Biegler [16] extended the method by using Lagrange polynomials instead of splines to approximate the state. In Cuthrell's method, the trajectory is divided into finite elements where global approximations are applied to each element individually. The state is then linked across elements, akin to state and control parameterization methods. Cuthrell and Biegler [16] also discussed equivalence, but did not focus on costate estimation, and hence did not explicitly formulate a mapping between the KKT multipliers of the NLP and the costate.

In this paper we develop a method for direct trajectory optimization and costate estimation called the *Gauss pseudospectral method* (GPM). It is noted that the Gauss pseudospectral method is based largely on [17], with extensions developed in [18], and has similarities with [16]. In the Gauss pseudospectral method, orthogonal collocation of the dynamics is performed at the LG points. The Gauss pseudospectral method differs from several other pseudospectral methods in that the dynamics are *not* collocated at the boundary points. This collocation, in conjunction with the proper approximation to the costate, leads to a set of KKT conditions that is *identical* to the discretized form of the first-order optimality conditions at the LG points. This equivalence between the KKT conditions and the discretized first-order necessary conditions leads to an accurate costate estimate using the KKT multipliers of the NLP. An example problem demonstrates the method's ability to obtain accurate estimates of the state, costate, and control for continuous-time optimal control problems. In particular, it is shown through the example that the errors in the state, costate, and control decrease rapidly as the number of discretization points increases. In addition, the Gauss pseudospectral method has been successfully implemented in multivehicle, multiphase trajectory optimization problems [18–20].

Received 11 October 2005; revision received 7 March 2006; accepted for publication 9 March 2006.

*Draper Laboratory Fellow; bensonda@alum.mit.edu.
†Draper Laboratory Fellow, Ph.D. Candidate, Department of Aeronautics and Astronautics, MIT; ghuntington@draper.com.
‡Distinguished Member of the Technical Staff, Tactical ISR Division; tomt@draper.com.
§Senior Member of the Technical Staff, Guidance, Navigation, and Control Systems Division; anilvrao@ufl.edu (corresponding author).

II. Continuous Bolza Problem

Without loss of generality, consider the following optimal control problem. Determine the state $\mathbf{x}(\tau) \in \mathbb{R}^n$, control $\mathbf{u}(\tau) \in \mathbb{R}^m$, initial time t_0, and final time t_f that minimize the cost functional

$$J = \Phi[\mathbf{x}(-1), t_0, \mathbf{x}(1), t_f] + \frac{t_f - t_0}{2}\int_{-1}^{1} g[\mathbf{x}(\tau), \mathbf{u}(\tau), \tau; t_0, t_f]\,\mathrm{d}\tau \tag{1}$$

subject to the constraints

$$\frac{\mathrm{d}\mathbf{x}}{\mathrm{d}\tau} = \frac{t_f - t_0}{2}\mathbf{f}[\mathbf{x}(\tau), \mathbf{u}(\tau), \tau; t_0, t_f] \tag{2}$$

$$\boldsymbol{\phi}\,[\mathbf{x}(-1), t_0, \mathbf{x}(1), t_f] = \mathbf{0} \in \mathbb{R}^q \tag{3}$$

$$\mathbf{C}\,[\mathbf{x}(\tau), \mathbf{u}(\tau), \tau; t_0, t_f] \leq \mathbf{0} \in \mathbb{R}^c \tag{4}$$

The optimal control problem of Eqs. (1–4) will be referred to as the *continuous Bolza problem*. It is noted that the optimal control problem of Eqs. (1–4) can be transformed from the time interval $\tau \in [-1, 1]$ to the time interval $t \in [t_0, t_f]$ via the affine transformation

$$t = \frac{t_f - t_0}{2}\tau + \frac{t_f + t_0}{2} \tag{5}$$

III. Gauss Pseudospectral Discretization of Continuous Bolza Problem

The direct approach to solving the continuous Bolza optimal control problem of Sec. II is to discretize and transcribe Eqs. (1–4) to a NLP. The Gauss pseudospectral method, like Legendre and Chebyshev methods, is based on approximating the state and control trajectories using interpolating polynomials. The state is approximated using a basis of $N+1$ Lagrange interpolating polynomials [21] L,

$$\mathbf{x}\,(\tau) \approx \mathbf{X}(\tau) = \sum_{i=0}^{N} \mathbf{X}(\tau_i) L_i(\tau) \tag{6}$$

where $L_i(\tau)$ $(i = 0, \ldots, N)$ are defined as

$$L_i(\tau) = \prod_{j=0, j\neq i}^{N} \frac{\tau - \tau_j}{\tau_i - \tau_j} \tag{7}$$

Additionally, the control is approximated using a basis of N Lagrange interpolating polynomials $L_i^*(\tau)$, $(i = 1, \ldots, N)$ as

$$\mathbf{u}\,(\tau) \approx \mathbf{U}(\tau) = \sum_{i=1}^{N} \mathbf{U}(\tau_i) L_i^*(\tau) \tag{8}$$

where

$$L_i^*(\tau) = \prod_{j=1, j\neq i}^{N} \frac{\tau - \tau_j}{\tau_i - \tau_j} \tag{9}$$

It can be seen from Eqs. (7) and (9) that $L_i(\tau)$ $(i = 0, \ldots, N)$ and $L_i^*(\tau)$ $(i = 1, \ldots, N)$ satisfy the properties

$$L_i(\tau_j) = \begin{cases} 1, & i = j \\ 0, & i \neq j \end{cases} \tag{10}$$

$$L_i^*(\tau_j) = \begin{cases} 1, & i = j \\ 0, & i \neq j \end{cases} \tag{11}$$

Differentiating the expression in Eq. (6), we obtain

$$\dot{\mathbf{x}}(\tau) \approx \dot{\mathbf{X}}(\tau) = \sum_{i=0}^{N} x(\tau_i)\dot{L}_i(\tau) \tag{12}$$

The derivative of each Lagrange polynomial at the LG points can be represented in a differential approximation matrix, $D \in \mathbb{R}^{N\times N+1}$. The elements of the differential approximation matrix are determined offline as follows:

$$D_{ki} = \dot{L}_i(\tau_k) = \sum_{l=0}^{N} \frac{\prod_{j=0, j\neq i,l}^{N}(\tau_k - \tau_j)}{\prod_{j=0, j\neq i}^{N}(\tau_i - \tau_j)} \tag{13}$$

where $k = 1, \ldots, N$ and $i = 0, \ldots, N$. The dynamic constraint is transcribed into algebraic constraints via the differential approximation matrix as follows:

$$\sum_{i=0}^{N} D_{ki}\mathbf{X}_i - \frac{t_f - t_0}{2}\mathbf{f}(\mathbf{X}_k, \mathbf{U}_k, \tau_k; t_0, t_f) = \mathbf{0} \qquad (k = 1, \ldots, N) \tag{14}$$

where $\mathbf{X}_k \equiv \mathbf{X}(\tau_k) \in \mathbb{R}^n$ and $\mathbf{U}_k \equiv \mathbf{U}(\tau_k) \in \mathbb{R}^m$ $(k = 1, \ldots, N)$. Note that the dynamic constraint is collocated only at the LG points and *not* at the boundary points (this form of collocation differs from other well-known pseudospectral methods such as those found in [9,10]). Additional variables in the discretization are defined as follows: $\mathbf{X}_0 \equiv \mathbf{X}(-1)$, and $\mathbf{X}_f$, where $\mathbf{X}_f$ is defined in terms of $\mathbf{X}_k$, $(k = 0, \ldots, N)$ and $\mathbf{U}_k$ $(k = 1, \ldots, N)$ via the Gauss quadrature [22]

$$\mathbf{X}_f \equiv \mathbf{X}_0 + \frac{t_f - t_0}{2}\sum_{k=1}^{N} w_k \mathbf{f}(\mathbf{X}_k, \mathbf{U}_k, \tau_k; t_0, t_f) \tag{15}$$

where w_k are the Gauss weights. The continuous cost function of Eq. (1) is approximated using a Gauss quadrature as

$$J = \Phi(\mathbf{X}_0, t_0, \mathbf{X}_f, t_f) + \frac{t_f - t_0}{2}\sum_{k=1}^{N} w_k g(\mathbf{X}_k, \mathbf{U}_k, \tau_k; t_0, t_f) \tag{16}$$

Next, the boundary constraint of Eq. (3) is expressed as

$$\boldsymbol{\phi}\,(\mathbf{X}_0, t_0, \mathbf{X}_f, t_f) = \mathbf{0} \tag{17}$$

Furthermore, the path constraint of Eq. (4) is evaluated at the LG points as

$$\mathbf{C}\,(\mathbf{X}_k, \mathbf{U}_k, \tau_k; t_0, t_f) \leq \mathbf{0} \qquad (k = 1, \ldots, N) \tag{18}$$

The cost function of Eq. (16) and the algebraic constraints of Eqs. (14), (15), (17), and (18) define an NLP whose solution is an approximate solution to the continuous Bolza problem. Finally, it is noted that discontinuities in the state or control can be handled efficiently by dividing the trajectory into *phases*, where the dynamics are transcribed within each phase and then connected together by additional phase interface (also known as *linkage*) constraints. This procedure has been used in many applications [17,19,20].

IV. KKT Conditions of the NLP

The first-order optimality conditions (i.e., the KKT conditions) of the NLP can be obtained using the augmented cost function or Lagrangian [23]. The augmented cost function is formed using the Lagrange multipliers $\tilde{\boldsymbol{\Lambda}}_k \in \mathbb{R}^n$, $\tilde{\boldsymbol{\mu}}_k \in \mathbb{R}^c$, $k = 1, \ldots, N$, $\tilde{\boldsymbol{\Lambda}}_F \in \mathbb{R}^n$, and $\tilde{\boldsymbol{\nu}} \in \mathbb{R}^q$ as

$$
\begin{aligned}
J_a = {} & \Phi(\mathbf{X}_0, t_0, \mathbf{X}_f, t_f) + \frac{t_f - t_0}{2}\sum_{k=1}^{N} w_k g(\mathbf{X}_k, \mathbf{U}_k, \tau_k; t_0, t_f) \\
& - \tilde{\boldsymbol{\nu}}^T \boldsymbol{\phi}(\mathbf{X}_0, t_0, \mathbf{X}_f, t_f) - \sum_{k=1}^{N} \tilde{\boldsymbol{\mu}}_k^T \mathbf{C}(\mathbf{X}_k, \mathbf{U}_k, \tau_k; t_0, t_f) \\
& - \sum_{k=1}^{N} \tilde{\boldsymbol{\Lambda}}_k^T \left(\sum_{i=0}^{N} D_{ki}\mathbf{X}_i - \frac{t_f - t_0}{2}\mathbf{f}(\mathbf{X}_k, \mathbf{U}_k, \tau_k; t_0, t_f) \right) \\
& - \tilde{\boldsymbol{\Lambda}}_F^T \left(\mathbf{X}_f - \mathbf{X}_0 - \frac{t_f - t_0}{2}\sum_{k=1}^{N} w_k \mathbf{f}(\mathbf{X}_k, \mathbf{U}_k, \tau_k; t_0, t_f) \right)
\end{aligned}
\tag{19}
$$

The KKT conditions are found by setting equal to zero the derivatives of the Lagrangian with respect to $\mathbf{X}_0, \mathbf{X}_k, \mathbf{X}_f, \mathbf{U}_k, \tilde{\boldsymbol{\Lambda}}_k, \tilde{\boldsymbol{\mu}}_k, \tilde{\boldsymbol{\Lambda}}_F, \tilde{\boldsymbol{\nu}}, t_0$, and t_f. The solution to the NLP of Sec. III must satisfy the following KKT conditions:

$$
\sum_{i=0}^{N} \mathbf{X}_i D_{ki} = \frac{t_f - t_0}{2}\mathbf{f}_k \tag{20}
$$

$$
\begin{aligned}
& -\sum_{i=1}^{N}\left(\frac{\tilde{\boldsymbol{\Lambda}}_i^T}{w_i} + \tilde{\boldsymbol{\Lambda}}_F^T\right)\frac{w_i}{w_k}D_{ik} + \tilde{\boldsymbol{\Lambda}}_F^T\sum_{i=1}^{N}\frac{w_i}{w_k}D_{ik} = \frac{t_f - t_0}{2}\left[-\frac{\partial g_k}{\partial \mathbf{X}_k}\right. \\
& \left. - \left(\frac{\tilde{\boldsymbol{\Lambda}}_k^T}{w_k} + \tilde{\boldsymbol{\Lambda}}_F^T\right)\frac{\partial \mathbf{f}_k}{\partial \mathbf{X}_k} + \frac{2}{t_f - t_0}\frac{\tilde{\boldsymbol{\mu}}_k^T}{w_k}\frac{\partial \mathbf{C}_k}{\partial \mathbf{X}_k}\right]
\end{aligned}
\tag{21}
$$

$$
\mathbf{0} = \frac{\partial g_k}{\partial \mathbf{U}_k} + \left(\frac{\tilde{\boldsymbol{\Lambda}}_k^T}{w_k} + \tilde{\boldsymbol{\Lambda}}_F^T\right)\frac{\partial \mathbf{f}_k}{\partial \mathbf{U}_k} - \frac{2}{t_f - t_0}\frac{\tilde{\boldsymbol{\mu}}_k^T}{w_k}\frac{\partial \mathbf{C}_k}{\partial \mathbf{U}_k} \tag{22}
$$

$$
\boldsymbol{\phi}\,(\mathbf{X}_0, t_0, \mathbf{X}_f, t_f) = \mathbf{0} \tag{23}
$$

$$
\tilde{\boldsymbol{\Lambda}}_0^T = -\frac{\partial \Phi}{\partial \mathbf{X}_0} + \tilde{\boldsymbol{\nu}}^T\frac{\partial \boldsymbol{\phi}}{\partial \mathbf{X}_0} \tag{24}
$$

$$
\tilde{\boldsymbol{\Lambda}}_F^T = \frac{\partial \Phi}{\partial \mathbf{X}_f} - \tilde{\boldsymbol{\nu}}^T\frac{\partial \boldsymbol{\phi}}{\partial \mathbf{X}_f} \tag{25}
$$

$$
-\frac{t_f - t_0}{2}\sum_{k=1}^{N} w_k\frac{\partial \tilde{\mathcal{H}}_k}{\partial t_0} + \frac{1}{2}\sum_{k=1}^{N} w_k\tilde{\mathcal{H}}_k = \frac{\partial \Phi}{\partial t_0} - \tilde{\boldsymbol{\nu}}^T\frac{\partial \boldsymbol{\phi}}{\partial t_0} \tag{26}
$$

$$
\frac{t_f - t_0}{2}\sum_{k=1}^{N} w_k\frac{\partial \tilde{\mathcal{H}}_k}{\partial t_f} + \frac{1}{2}\sum_{k=1}^{N} w_k\tilde{\mathcal{H}}_k = -\frac{\partial \Phi}{\partial t_f} + \tilde{\boldsymbol{\nu}}^T\frac{\partial \boldsymbol{\phi}}{\partial t_f} \tag{27}
$$

$$
\mathbf{C}_k \le \mathbf{0} \tag{28}
$$

$$
\tilde{\mu}_{jk} = 0, \quad \text{when } C_{jk} < 0 \tag{29}
$$

$$
\tilde{\mu}_{jk} \le 0, \quad \text{when } C_{jk} = 0 \tag{30}
$$

$$
\mathbf{X}_f = \mathbf{X}_0 + \frac{(t_f - t_0)}{2}\sum_{k=1}^{N} w_k\mathbf{f}_k \tag{31}
$$

$$
\begin{aligned}
\tilde{\boldsymbol{\Lambda}}_F = {} & \tilde{\boldsymbol{\Lambda}}_0 + \frac{t_f - t_0}{2}\sum_{k=1}^{N} w_k\left[-\frac{\partial g_k}{\partial \mathbf{X}_k} - \left(\frac{\tilde{\boldsymbol{\Lambda}}_k^T}{w_k} + \tilde{\boldsymbol{\Lambda}}_F^T\right)\frac{\partial \mathbf{f}_k}{\partial \mathbf{X}_k}\right. \\
& \left. + \frac{2}{t_f - t_0}\frac{\tilde{\boldsymbol{\mu}}_k^T}{w_k}\frac{\partial \mathbf{C}_k}{\partial \mathbf{X}_k}\right]
\end{aligned}
\tag{32}
$$

where the shorthand notation $g_k \equiv g(\mathbf{X}_k, \mathbf{U}_k, \tau_k; t_0, t_f)$, $\mathbf{f}_k \equiv \mathbf{f}(\mathbf{X}_k, \mathbf{U}_k, \tau_k; t_0, t_f)$, $\tilde{\mathcal{H}}_k \equiv \tilde{\mathcal{H}}(\mathbf{X}_k, \tilde{\boldsymbol{\Lambda}}_k, \tilde{\boldsymbol{\Lambda}}_F, \tilde{\boldsymbol{\mu}}_k, \mathbf{U}_k, \tau_k; t_0, t_f)$, and $C_{jk} \equiv C_j(\mathbf{X}_k, \mathbf{U}_k, \tau_k; t_0, t_f)$ is used and $\tilde{\mu}_{jk}$ is the jth component of the $\tilde{\boldsymbol{\mu}}_k$. Note that the augmented Hamiltonian $\tilde{\mathcal{H}}_k$ is defined as

$$
\tilde{\mathcal{H}}_k \equiv g_k + \left(\frac{\tilde{\boldsymbol{\Lambda}}_k^T}{w_k} + \tilde{\boldsymbol{\Lambda}}_F^T\right)\mathbf{f}_k - \frac{2}{t_f - t_0}\frac{\tilde{\boldsymbol{\mu}}_k^T}{w_k}\mathbf{C}_k \tag{33}
$$

and $\tilde{\boldsymbol{\Lambda}}_0$ is defined as

$$
\tilde{\boldsymbol{\Lambda}}_0^T \equiv -\frac{\partial \Phi}{\partial \mathbf{X}_0} + \tilde{\boldsymbol{\nu}}^T\frac{\partial \boldsymbol{\phi}}{\partial \mathbf{X}_0} \tag{34}
$$

V. First-Order Necessary Conditions of the Continuous Bolza Problem

The indirect approach to solving the continuous Bolza problem of Eqs. (1–4) in Sec. II is to apply the calculus of variations and Pontryagin's maximum principle [24] to obtain first-order necessary conditions for optimality [2]. These variational conditions are typically derived using the augmented Hamiltonian $\mathcal{H}$ defined as

$$
\begin{aligned}
\mathcal{H}(\mathbf{x}, \boldsymbol{\lambda}, \boldsymbol{\mu}, \mathbf{u}, \tau; t_0, t_f) = {} & g(\mathbf{x}, \mathbf{u}, \tau; t_0, t_f) + \boldsymbol{\lambda}^T(\tau)\mathbf{f}(\mathbf{x}, \mathbf{u}, \tau; t_0, t_f) \\
& - \boldsymbol{\mu}^T(\tau)\mathbf{C}(\mathbf{x}, \mathbf{u}, \tau; t_0, t_f)
\end{aligned}
\tag{35}
$$

where $\boldsymbol{\lambda}(\tau) \in \mathbb{R}^n$ is the costate and $\boldsymbol{\mu}(\tau) \in \mathbb{R}^c$ is the Lagrange multiplier associated with the path constraint. The continuous-time first-order optimality conditions can be shown to be

$$
\frac{d\mathbf{x}}{d\tau} = \frac{t_f - t_0}{2}\mathbf{f}(\mathbf{x}, \mathbf{u}, \tau; t_0, t_f) = \frac{t_f - t_0}{2}\frac{\partial \mathcal{H}}{\partial \boldsymbol{\lambda}}
$$

$$
\frac{d\boldsymbol{\lambda}}{d\tau} = \frac{t_f - t_0}{2}\left(-\frac{\partial g}{\partial \mathbf{x}} - \boldsymbol{\lambda}^T\frac{\partial \mathbf{f}}{\partial \mathbf{x}} + \boldsymbol{\mu}^T\frac{\partial \mathbf{C}}{\partial \mathbf{x}}\right) = -\frac{t_f - t_0}{2}\frac{\partial \mathcal{H}}{\partial \mathbf{x}}
$$

$$
\mathbf{0} = \frac{\partial g}{\partial \mathbf{u}} + \boldsymbol{\lambda}^T\frac{\partial \mathbf{f}}{\partial \mathbf{u}} - \boldsymbol{\mu}^T\frac{\partial \mathbf{C}}{\partial \mathbf{u}} = \frac{\partial \mathcal{H}}{\partial \mathbf{u}}
$$

$$
\boldsymbol{\phi}\,[\mathbf{x}(\tau_0), t_0, \mathbf{x}(\tau_f), t_f] = \mathbf{0} \tag{36}
$$

$$
\boldsymbol{\lambda}(\tau_0) = -\frac{\partial \Phi}{\partial \mathbf{x}(\tau_0)} + \boldsymbol{\nu}^T\frac{\partial \phi}{\partial \mathbf{x}(\tau_0)}, \qquad \boldsymbol{\lambda}(\tau_f) = \frac{\partial \Phi}{\partial \mathbf{x}(\tau_f)} - \boldsymbol{\nu}^T\frac{\partial \boldsymbol{\phi}}{\partial \mathbf{x}(\tau_f)}
$$

$$
\mathcal{H}(t_0) = \frac{\partial \Phi}{\partial t_0} - \boldsymbol{\nu}^T\frac{\partial \boldsymbol{\phi}}{\partial t_0}, \qquad \mathcal{H}(t_f) = -\frac{\partial \Phi}{\partial t_f} + \boldsymbol{\nu}^T\frac{\partial \boldsymbol{\phi}}{\partial t_f}
$$

$$
\mu_j(\tau) = 0, \text{ when } C_j(\mathbf{x}, \mathbf{u}, \tau; t_0, t_f) < 0, \quad j = 1, \ldots, c
$$

$$
\mu_j(\tau) \le 0, \text{ when } C_j(\mathbf{x}, \mathbf{u}, \tau; t_0, t_f) = 0, \quad j = 1, \ldots, c
$$

where $\boldsymbol{\nu} \in \mathbb{R}^q$ is the Lagrange multiplier associated with the boundary condition $\boldsymbol{\phi}$. It can be shown that the augmented Hamiltonian at the initial and final times can be written, respectively, as

$$
\mathcal{H}(t_0) = -\frac{t_f - t_0}{2}\int_{-1}^{1}\frac{\partial \mathcal{H}}{\partial t_0}\,d\tau + \frac{1}{2}\int_{-1}^{1}\mathcal{H}\,d\tau \tag{37}
$$

$$
\mathcal{H}(t_f) = \frac{t_f - t_0}{2}\int_{-1}^{1}\frac{\partial \mathcal{H}}{\partial t_f}\,d\tau + \frac{1}{2}\int_{-1}^{1}\mathcal{H}\,d\tau \tag{38}
$$

VI. Gauss Pseudospectral Discretized Necessary Conditions

To discretize the variational conditions of Sec. V using the Gauss pseudospectral discretization, it is necessary to form an appropriate approximation for the costate. In this method, the costate $\boldsymbol{\lambda}(\tau)$ is approximated as follows:

$$\boldsymbol{\lambda}(\tau) \approx \boldsymbol{\Lambda}(\tau) = \sum_{i=1}^{N+1} \boldsymbol{\lambda}(\tau_i) L_i^\dagger(\tau) \tag{39}$$

where $L_i^\dagger(\tau)$ $(i = 1, \ldots, N+1)$ are defined as

$$L_i^\dagger(\tau) = \prod_{j=1, j\neq i}^{N+1} \frac{\tau - \tau_j}{\tau_i - \tau_j} \tag{40}$$

It is emphasized that the costate approximation is *different* from the state approximation. In particular, the basis of $N+1$ Lagrange interpolating polynomials $L_i^\dagger(\tau)$ $(i = 1, \ldots, N+1)$ includes the costate at the *final* time (as opposed to the initial time which is used in the state approximation). This (nonintuitive) costate approximation is necessary to provide a complete mapping between the KKT conditions and the variational conditions. Some other useful relationships involve the derivative of the costate approximation as follows [17]:

$$\begin{aligned} \dot{L}_i^\dagger(\tau_k) &= D_{ki}^\dagger = -\frac{w_i}{w_k} D_{ik}, \qquad i, k = 1, \ldots, N \\ \dot{L}_{N+1}^\dagger(\tau_k) &= D_{k,N+1}^\dagger = \sum_{i=1}^{N} \frac{w_i}{w_k} D_{ik}, \qquad k = 1, \ldots, N \end{aligned} \tag{41}$$

Using the costate approximation of Eq. (39), the first-order necessary conditions of the continuous Bolza problem in Eq. (36) are discretized as follows. First, the state and control are approximated using Eqs. (6) and (8), respectively. Next, the costate is approximated using the basis of $N+1$ Lagrange interpolating polynomials as defined in Eq. (39). The continuous-time first-order optimality conditions of Eq. (36) are discretized using the variables $\mathbf{X}_0 \equiv \mathbf{X}(-1)$, $\mathbf{X}_k \equiv \mathbf{X}(\tau_k) \in \mathbb{R}^n$, and $\mathbf{X}_f \equiv \mathbf{X}(1)$ for the state, $\mathbf{U}_k \equiv \mathbf{U}(\tau_k) \in \mathbb{R}^m$ for the control, $\boldsymbol{\Lambda}_0 \equiv \boldsymbol{\Lambda}(-1)$, $\boldsymbol{\Lambda}_k \equiv \boldsymbol{\Lambda}(\tau_k) \in \mathbb{R}^n$, and $\boldsymbol{\Lambda}_f \equiv \boldsymbol{\Lambda}(1)$ for the costate, and $\boldsymbol{\mu}_k \equiv \boldsymbol{\mu}(\tau_k) \in \mathbb{R}^c$ for the Lagrange multiplier associated with the path constraints at the LG points $k = 1, \ldots, N$. The other unknown variables in the problem are the initial and final times, $t_0 \in \mathbb{R}$, $t_f \in \mathbb{R}$, and the Lagrange multiplier $\boldsymbol{\nu} \in \mathbb{R}^q$. The total number of variables is then given as $(2n+m+c)N + 4n + q + 2$. These variables are used to discretize the continuous necessary conditions of Eq. (36) via the Gauss pseudospectral discretization. Note that the derivative of the state is approximated using Lagrange polynomials based on $N+1$ points consisting of the N LG points and the initial time τ_0, whereas the derivative of the costate is approximated using Lagrange polynomials based on $N+1$ points consisting of the N LG points and the final time τ_f. The resulting algebraic equations that approximate the continuous necessary conditions at the LG points are given as

$$\sum_{i=0}^{N} \mathbf{X}_i D_{ki} = \frac{t_f - t_0}{2} \mathbf{f}_k \tag{42}$$

$$\sum_{i=1}^{N} \boldsymbol{\Lambda}_i D_{ki}^\dagger + \boldsymbol{\Lambda}_f D_{k,N+1}^\dagger = \frac{t_f - t_0}{2}\left(-\frac{\partial g_k}{\partial \mathbf{X}_k} - \boldsymbol{\Lambda}_k^T \frac{\partial \mathbf{f}_k}{\partial \mathbf{X}_k} + \boldsymbol{\mu}_k^T \frac{\partial \mathbf{C}_k}{\partial \mathbf{X}_k}\right) \tag{43}$$

$$\mathbf{0} = \frac{\partial g_k}{\partial \mathbf{U}_k} + \boldsymbol{\Lambda}_k^T \frac{\partial \mathbf{f}_k}{\partial \mathbf{U}_k} - \boldsymbol{\mu}_k^T \frac{\partial \mathbf{C}_k}{\partial \mathbf{U}_k} \tag{44}$$

$$\boldsymbol{\phi}(\mathbf{X}_0, t_0, \mathbf{X}_f, t_f) = \mathbf{0} \tag{45}$$

$$\boldsymbol{\Lambda}_0^T = -\frac{\partial \Phi}{\partial \mathbf{X}_0} + \boldsymbol{\nu}^T \frac{\partial \boldsymbol{\phi}}{\partial \mathbf{X}_0} \tag{46}$$

$$\boldsymbol{\Lambda}_f^T = \frac{\partial \Phi}{\partial \mathbf{X}_f} - \boldsymbol{\nu}^T \frac{\partial \boldsymbol{\phi}}{\partial \mathbf{X}_f} \tag{47}$$

$$-\frac{t_f - t_0}{2} \sum_{k=1}^{N} w_k \frac{\partial \mathcal{H}_k}{\partial t_0} + \frac{1}{2} \sum_{k=1}^{N} w_k \mathcal{H}_k = \frac{\partial \Phi}{\partial t_0} - \boldsymbol{\nu}^T \frac{\partial \boldsymbol{\phi}}{\partial t_0} \tag{48}$$

$$\frac{t_f - t_0}{2} \sum_{k=1}^{N} w_k \frac{\partial \mathcal{H}_k}{\partial t_f} + \frac{1}{2} \sum_{k=1}^{N} w_k \mathcal{H}_k = -\frac{\partial \Phi}{\partial t_f} + \boldsymbol{\nu}^T \frac{\partial \boldsymbol{\phi}}{\partial t_f} \tag{49}$$

$$\mu_{jk} = 0, \quad \text{when } C_{jk} < 0 \tag{50}$$

$$\mu_{jk} \leq 0, \quad \text{when } C_{jk} = 0 \tag{51}$$

for $k = 1, \ldots, N$ and $j = 1, \ldots, c$. The final two equations that are required (to link the initial and final state and costate, respectively) are

$$\mathbf{X}_f = \mathbf{X}_0 + \frac{t_f - t_0}{2} \sum_{k=1}^{N} w_k \mathbf{f}_k \tag{52}$$

$$\boldsymbol{\Lambda}_f = \boldsymbol{\Lambda}_0 + \frac{t_f - t_0}{2} \sum_{k=1}^{N} w_k \left(-\frac{\partial g_k}{\partial \mathbf{X}_k} - \boldsymbol{\Lambda}_k^T \frac{\partial \mathbf{f}_k}{\partial \mathbf{X}_k} + \boldsymbol{\mu}_k^T \frac{\partial \mathbf{C}_k}{\partial \mathbf{X}_k}\right) \tag{53}$$

The total number of equations in the set of discrete necessary conditions of Eqs. (42–53) is $(2n+m+c)N + 4n + q + 2$ (the same number of unknown variables). Solving these nonlinear algebraic equations would be an indirect solution to the optimal control problem.

VII. Costate Estimate

Using the results of Secs. IV and VI, a costate estimate for the continuous Bolza problem can be obtained at the LG points and the boundary points. This costate estimate is summarized via the following theorem:

Theorem 1 (Gauss pseudospectral costate mapping theorem): The KKT conditions of the NLP are exactly equivalent to the discretized form of the continuous first-order necessary conditions of the continuous Bolza problem when using the Gauss pseudospectral discretization. Furthermore, a costate estimate at the initial time, final time, and the Legendre–Gauss points can be found from the KKT multipliers, $\tilde{\boldsymbol{\Lambda}}_k$, $\tilde{\boldsymbol{\mu}}_k$, $\tilde{\boldsymbol{\Lambda}}_F$, and $\tilde{\boldsymbol{\nu}}$,

$$\begin{gathered} \boldsymbol{\Lambda}_k = \frac{\tilde{\boldsymbol{\Lambda}}_k}{w_k} + \tilde{\boldsymbol{\Lambda}}_F, \qquad \boldsymbol{\mu}_k = \frac{2}{t_f - t_0} \frac{\tilde{\boldsymbol{\mu}}_k}{w_k}, \qquad \boldsymbol{\nu} = \tilde{\boldsymbol{\nu}} \\ \boldsymbol{\Lambda}(t_0) = \tilde{\boldsymbol{\Lambda}}_0, \qquad \boldsymbol{\Lambda}(t_f) = \tilde{\boldsymbol{\Lambda}}_F \end{gathered} \tag{54}$$

Proof of Theorem 1: Using the substitution of Eq. (54), it is seen that Eqs. (20–32) are exactly the same as Eqs. (42–53).

Theorem 1 indicates that solving the NLP derived from the Gauss pseudospectral transcription of the optimal control problem is equivalent to applying the Gauss pseudospectral discretization to the continuous-time variational conditions. Figure 1 shows the solution path for both the direct and indirect methods.

VIII. Application of Gauss Pseudospectral Method

Consider the following optimal control problem. Minimize the cost functional

$$J = \frac{1}{2} \int_0^{t_f} (y + u^2)\, \mathrm{d}t \tag{55}$$

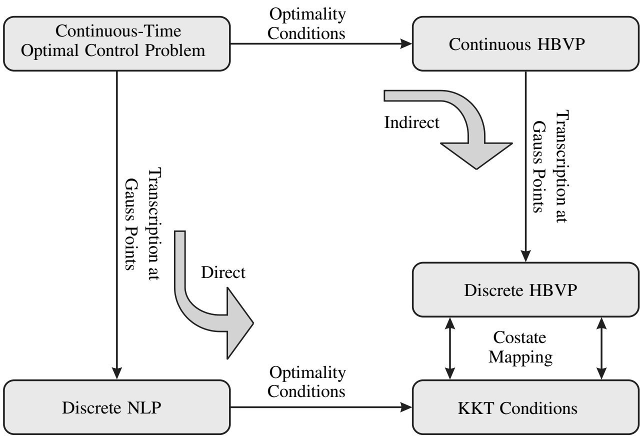

Fig. 1 Gauss pseudospectral discretization.

subject to the dynamic constraint

$$\dot{y} = 2y + 2u\sqrt{y} \tag{56}$$

and the boundary conditions

$$y(0) = a, \qquad y(t_f) = b \tag{57}$$

where $y(t) \in \mathbb{R}^+$ and $u(t) \in \mathbb{R}$ are the state and control, respectively, and t_f is fixed. It is noted that the optimal control problem of Eqs. (55–57) was derived from a standard linear quadratic (LQ) optimal control problem via a monotonic transformation $y(t) = x^2(t)$ [where $x(t)$ is the state of the LQ problem] and, thus, has an analytic solution.

The optimal control problem of Eqs. (55–57) was transcribed to an NLP using the Gauss pseudospectral discretization of Sec. III. The NLP was solved using the TOMLAB™ version of the NLP solver SNOPT [25,26] using default optimality and feasibility tolerances and using the following number of LG points: $N = [5, 6, \ldots, 40]$. The GPM solutions for the state, control, and costate for $N = 40$ are shown in Fig. 2 alongside the exact solution. It is noted that the maximum absolute errors in the state, costate, and control (over all nodes $\tau_0, \ldots, \tau_{N+1}$) are approximately 9×10^{-7}, 1.23×10^{-5}, and 4.2×10^{-6}, respectively. Next, let ϵ_Y and ϵ_Λ be the maximum absolute errors between the GPM and exact solutions over all nodes $\tau_0, \ldots, \tau_{N+1}$, and let ϵ_{Λ_0} be absolute error in the initial costate. Figure 3 shows the errors in the state, costate, and initial costate for $N \in [5, \ldots, 40]$. It is seen from Fig. 3 that the error in the state decreases to near the level of the feasibility and optimality tolerances specified in the NLP solver ($\approx 10^{-6}$). It is interesting to observe that, for this problem, the GPM appears to exhibit spectral convergence [27] (i.e., the error decreases faster than any power of $1/N$) until the value $N = 20$ (where the optimality and feasibility tolerances are reached), and that the initial costate converges faster than either the state or costate at the LG points.

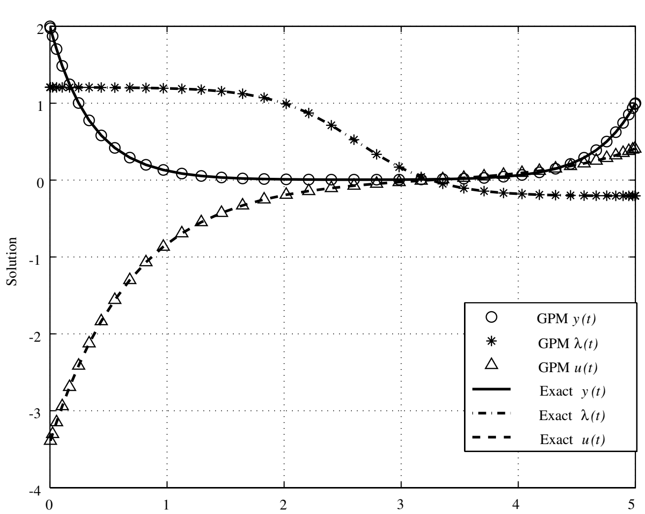

Fig. 2 Solution to example for $N = 40$.

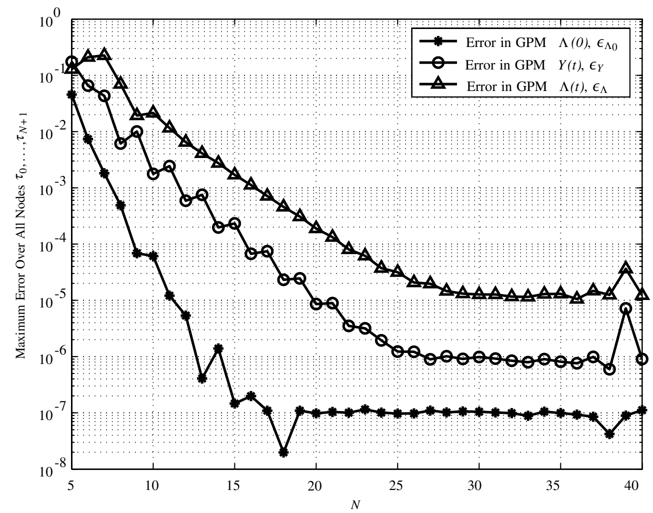

Fig. 3 Error in GPM solution for example as a function of N.

IX. Conclusions

A pseudospectral method, called the Gauss pseudospectral method, has been described for solving optimal control problems numerically. In this method the dynamics are collocated at a set of Legendre–Gauss points. It was shown that the KKT conditions from the NLP obtained via the Gauss pseudospectral discretization are identical to the variational conditions of the continuous-time optimal control problem discretized via the Gauss pseudospectral method. As a result, the KKT multipliers of the NLP can be used to obtain an accurate estimate of the costate at both the Legendre–Gauss points and the boundary points. The method was demonstrated on an example problem. It is shown that the errors in the state, costate, and control decrease rapidly as the number of collocation points increases. The results obtained in this paper demonstrate the viability of the Gauss pseudospectral method as a means of obtaining accurate solutions to continuous-time optimal control problems.

Acknowledgments

This research was funded in part by the Charles Stark Draper Laboratory, Inc., under internal research and development funds, and by the NASA Goddard Spaceflight Center under Cooperative Agreement NAS5-NCC5-730. The authors would like to acknowledge Matt Bottkol and Ron Proulx for their insight, guidance, and helpful suggestions.

References

[1] Betts, J. T., "Survey of Numerical Methods for Trajectory Optimization," *Journal of Guidance, Control, and Dynamics*, Vol. 21, No. 2, 1998, pp. 193–207.

[2] Kirk, D. E., *Optimal Control Theory: An Introduction*, Prentice–Hall, Upper Saddle River, NJ, 1970.

[3] Kraft, D., "On Converting Optimal Control Problems into Nonlinear Programming Codes," *Computational Mathematical Programming*, edited by K. Schittkowski, Vol. 15, NATO ASI Series, Springer, New York, 1985, pp. 261–280.

[4] Hargraves, C. R., and Paris, S. W., "Direct Trajectory Optimization Using Nonlinear Programming and Collocation," *Journal of Guidance, Control, and Dynamics*, Vol. 10, No. 4, 1987, pp. 338–342.

[5] Betts, J. T., *Practical Methods for Optimal Control Using Nonlinear Programming*, SIAM Press, Philadelphia, PA, 2001.

[6] Enright, P. J., and Conway, B. A., "Discrete Approximations to Optimal Trajectories Using Direct Transcription and Nonlinear Programming," *Journal of Guidance, Control, and Dynamics*, Vol. 15, No. 4, 1992, pp. 994–1002.

[7] Vlassenbroeck, J., and Van Doreen, R., "A Chebyshev Technique for Solving Nonlinear Optimal Control Problems," *IEEE Transactions on Automatic Control*, Vol. 33, No. 4, 1988, pp. 333–340.

[8] Vlassenbroeck, J., "A Chebyshev Polynomial Method for Optimal Control with State Constraints," *Automatica*, Vol. 24, No. 4, 1988, pp. 499–506.

[9] Elnagar, G., Kazemi, M., and Razzaghi, M., "The Pseudospectral Legendre Method for Discretizing Optimal Control Problems," *IEEE Transactions on Automatic Control*, Vol. 40, No. 10, 1995, pp. 1793–1796.

[10] Elnagar, G., and Kazemi, M., "Pseudospectral Chebyshev Optimal Control of Constrained Nonlinear Dynamical Systems," *Computational Optimization and Applications*, Vol. 11, No. 2, 1998, pp. 195–217.

[11] Canuto, C., Hussaini, M. Y., Quarteroni, A., and Zang, T. A., *Spectral Methods in Fluid Dynamics*, Springer–Verlag, New York, 1988.

[12] Fornberg, B., *A Practical Guide to Pseudospectral Methods*, Cambridge Univ. Press, New York, 1998.

[13] Fahroo, F., and Ross, I. M., "Costate Estimation by a Legendre Pseudospectral Method," *Journal of Guidance, Control, and Dynamics*, Vol. 24, No. 2, 2001, pp. 270–277.

[14] Ross, I. M., and Fahroo, F., "Legendre Pseudospectral Approximations of Optimal Control Problems," *Lecture Notes in Control and Information Sciences*, Springer–Verlag, New York, 2003.

[15] Reddien, G. W., "Collocation at Gauss Points as a Discretization in Optimal Control," *SIAM Journal of Control and Optimization*, Vol. 17, No. 2, March 1979, pp. 298–306.

[16] Cuthrell, J. E., and Biegler, L. T., "Simultaneous Optimization and Solution Methods for Batch Reactor Control Profiles," *Computers and Chemical Engineering*, Vol. 13, No. 1/2, 1989, pp. 49–62.

[17] Benson, D., "A Gauss Pseudospectral Transcription for Optimal Control," Ph.D. Thesis, Department of Aeronautics and Astronautics, MIT, Nov. 2004.

[18] Huntington, G. T., Benson, D. A., and Rao, A. V., "Post-Optimality Evaluation and Analysis of a Formation Flying Problem via a Gauss Pseudospectral Method," AAS Paper 05-339, 2005.

[19] Huntington, G. T., and Rao, A. V., "Optimal Spacecraft Formation Configuration Using a Gauss Pseudospectral Method," AAS Paper 05-103, 2005.

[20] Huntington, G. T., and Rao, A. V., "Optimal Reconfiguration of a Spacecraft Formation via a Gauss Pseudospectral Method," AAS Paper 05-338, 2005.

[21] Davis, P., *Interpolation & Approximation*, Dover, New York, 1975.

[22] Davis, P., and Rabinowitz, P., *Methods of Numerical Integration*, Academic Press, New York, 1984.

[23] Bertsekas, D., *Nonlinear Programming*, Athena Scientific, Belmont, MA, 1995.

[24] Pontryagin, L. S., Boltyanskii, V., Gamkrelidze, R., and Mischenko, E., *The Mathematical Theory of Optimal Processes*, Interscience, New York, 1962.

[25] Gill, P. E., Murray, W., and Saunders, M. A., "SNOPT: An SQP Algorithm for Large Scale Constrained Optimization," *SIAM Journal on Optimization*, Vol. 12, No. 4, 2002, pp. 979–1006.

[26] Holmstrom, K., Goran, A. O., and Edvall, M. M., "*User's Guide for TOMLAB/SNOPT*," TOMLAB Optimization, 2005, http://tomlab.biz.

[27] Gottlieb, D., and Orszag, S., *Numerical Analysis of Spectral Methods: Theory and Applications*, Society for Industrial and Applied Mathematics, Philadelphia, 1977.